

## Supporting Information:

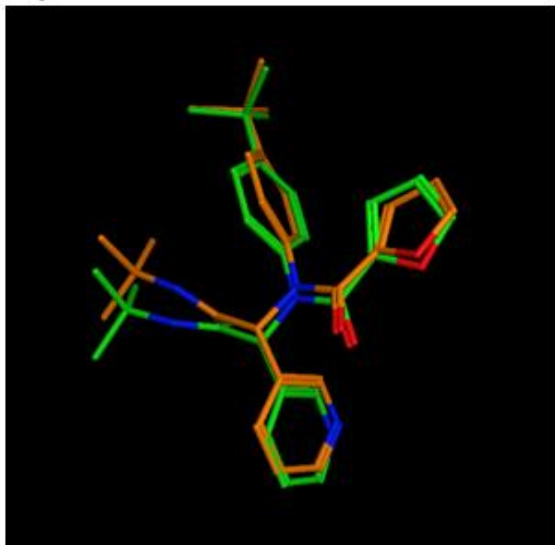
### Repurposing approved Drugs as potential Inhibitors of 3CL- protease of SARS-CoV-2: Virtual screening and Structure Based Drug Design

*Franz-Josef Meyer-Almes\**

Department of Chemical Engineering and Biotechnology, University of Applied Sciences  
Darmstadt, Haardtring 100, 64295 Darmstadt, Germany.

Email: [franz-josef.meyer-almes@h-da.de](mailto:franz-josef.meyer-almes@h-da.de)

**A)**



**B)**

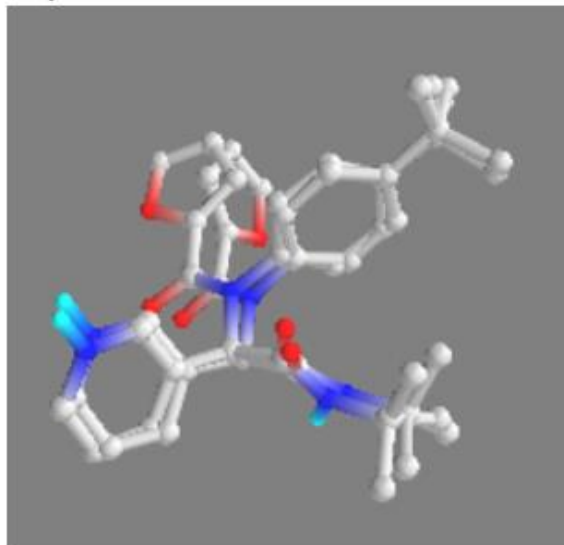
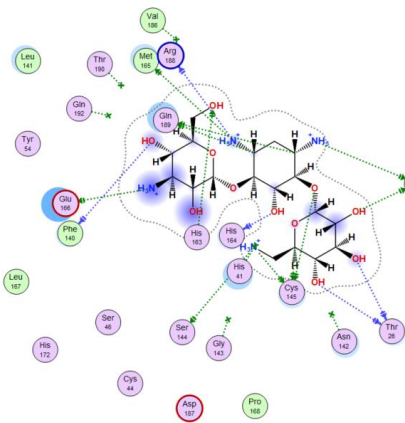
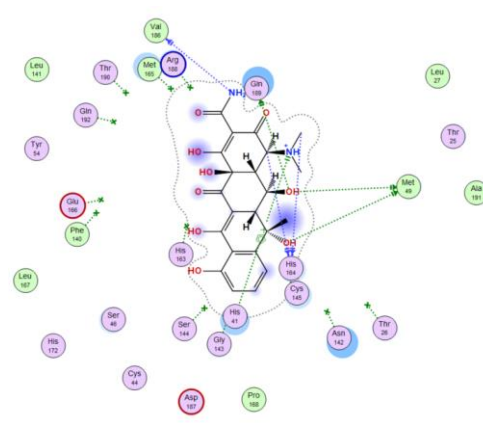


Fig. S1: Redocking of non-covalent ligand ML188 into the crystal structure of 3CL<sup>pro</sup> (PDB-ID: 3V3M) using A) MOE (AMBER 14 force field) and B) Autodock Vina yielding RMSD-values of 0.981 Å and 0.926 Å.

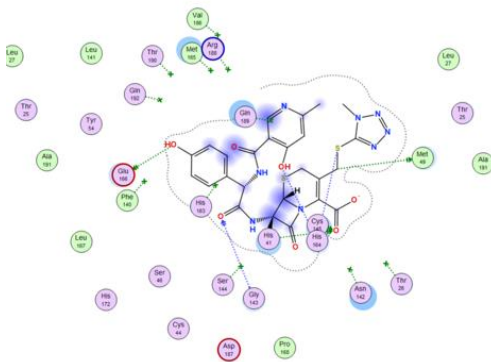
A)



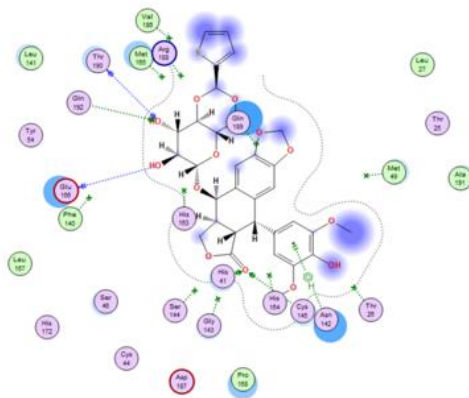
B)



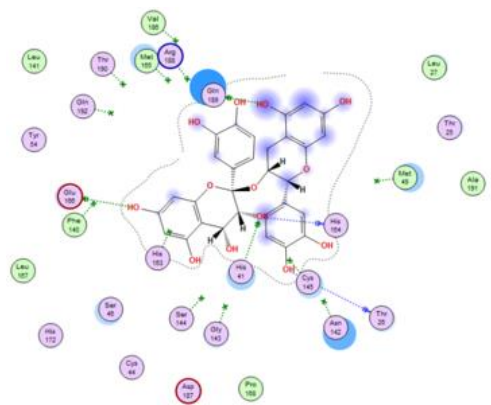
C)



D)



E)



F)

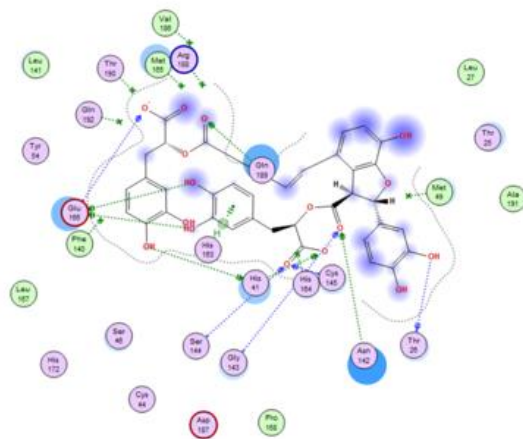


Fig. S2: Ligand interactions of A) Kanamycin, B) Oxytetracycline, C) Cefpiramide, D) Teniposide, E) Proanthocyanidins and F) Salvianolic acid B

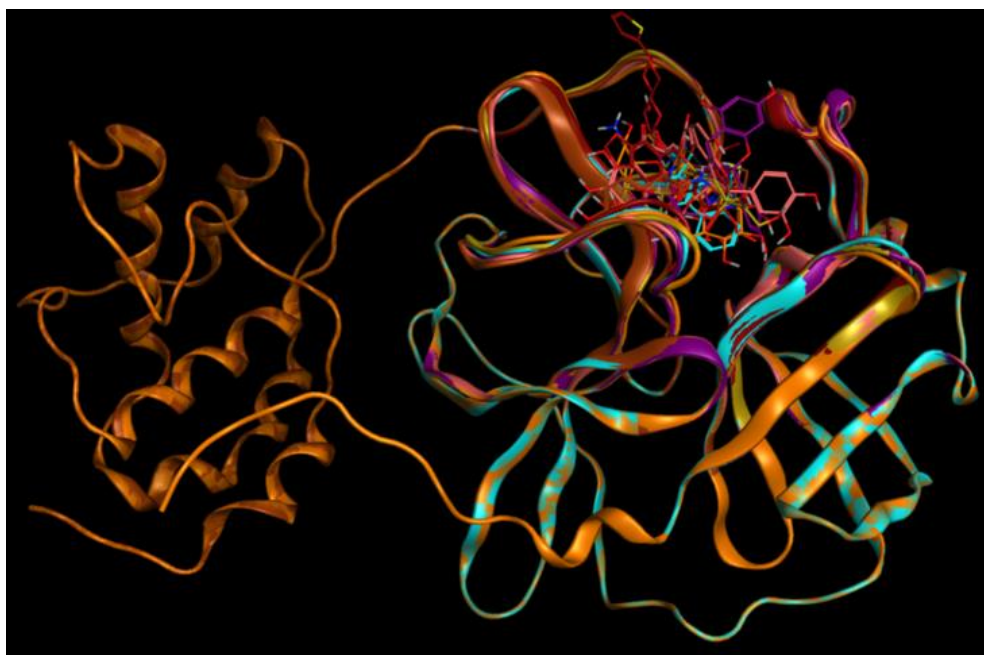


Fig. S3: Overlay of docked (induced fit) and energy minimized complexes between 3CLpro (PDB-ID: 6LU7) and the following ligands: Kanamycin, Oxytetracycline, Cefpiramide, Doxorubicin, Teniposide, Proanthocyanidins, Salvianolic acid B. All ligands dock into the conservative active site of the cysteine protease.

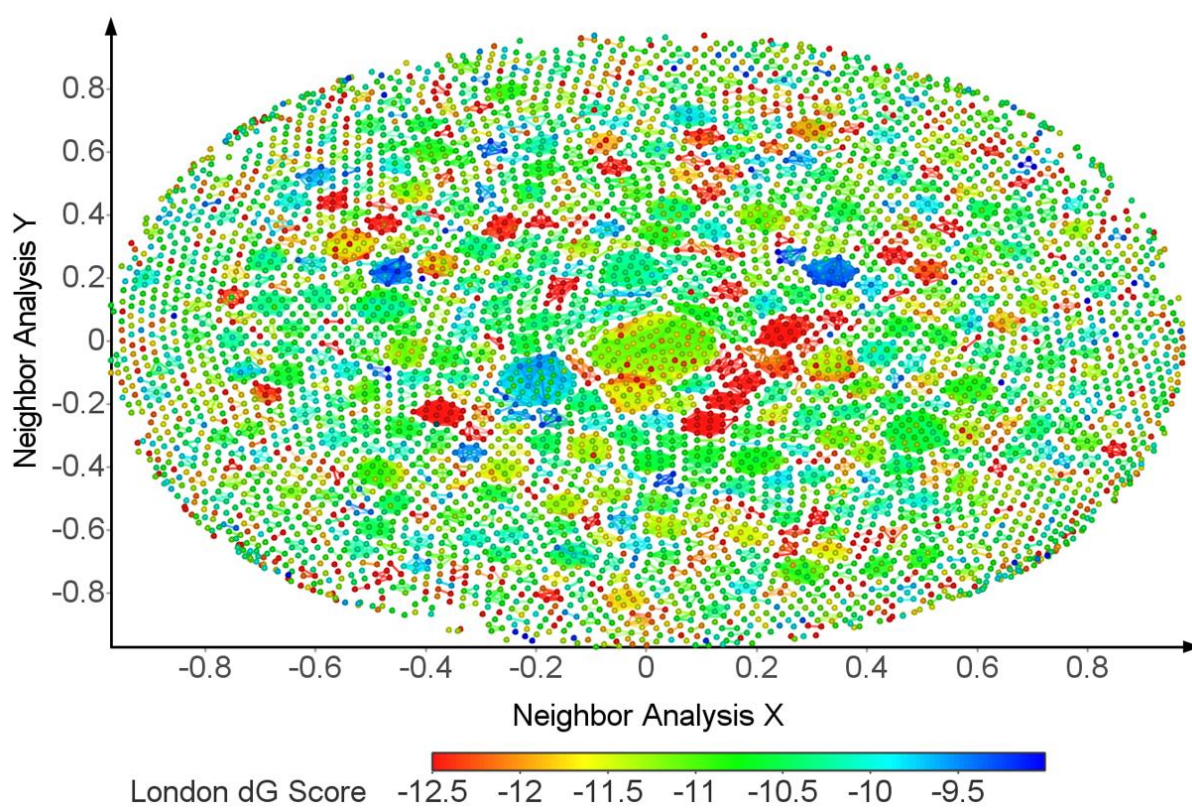


Fig. S4: Similarity/Activity cliff analysis of 5517 hits from the pharmacophore search of ZINC15 library demonstrating several clusters of similar chemical structures with high docking scores ( $< -11.5$ ).

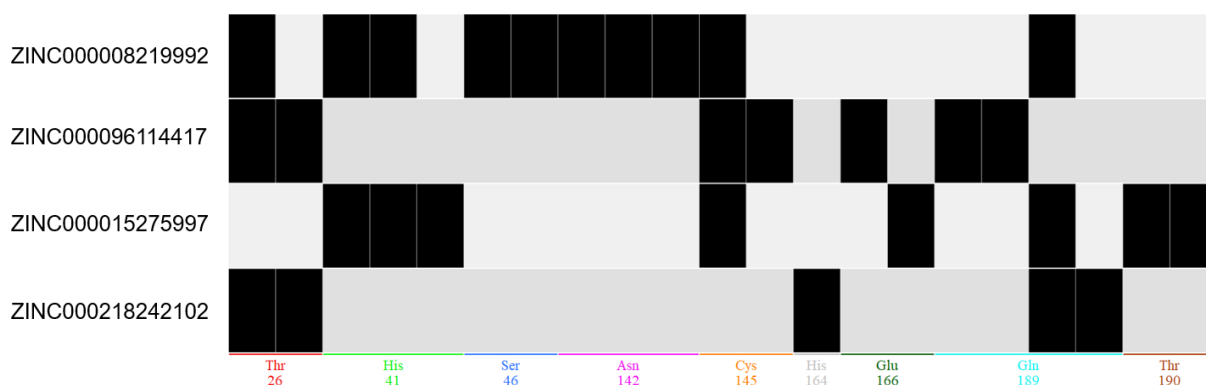


Fig. S5: Different patterns of protein-ligand interaction fingerprints (PLIFs) of best scoring hits from pharmacophore search against ZINC15 library within the active site of 3CL<sup>pro</sup>.

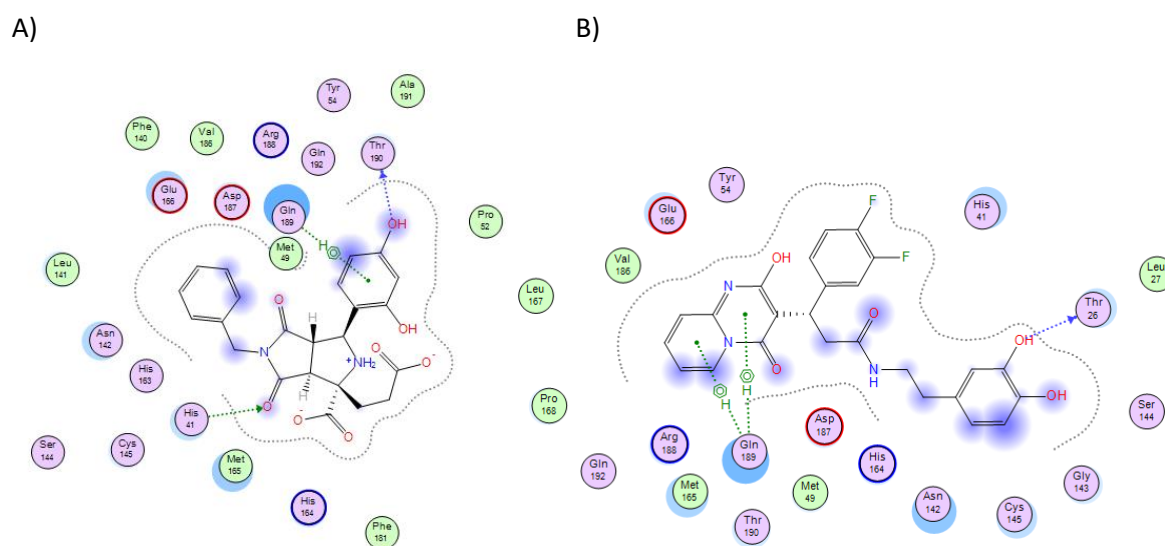


Fig. S6: 2D protein-ligand interactions between 3CL<sup>pro</sup> of SARS-CoV-2 and A) ZINC000015275997 and B) ZINC000218242102. There are new opportunities for aliphatic-aromatic interactions with Gln189 and H-bond-interactions with Thr190.

Starting point:  
Oxytetracycline

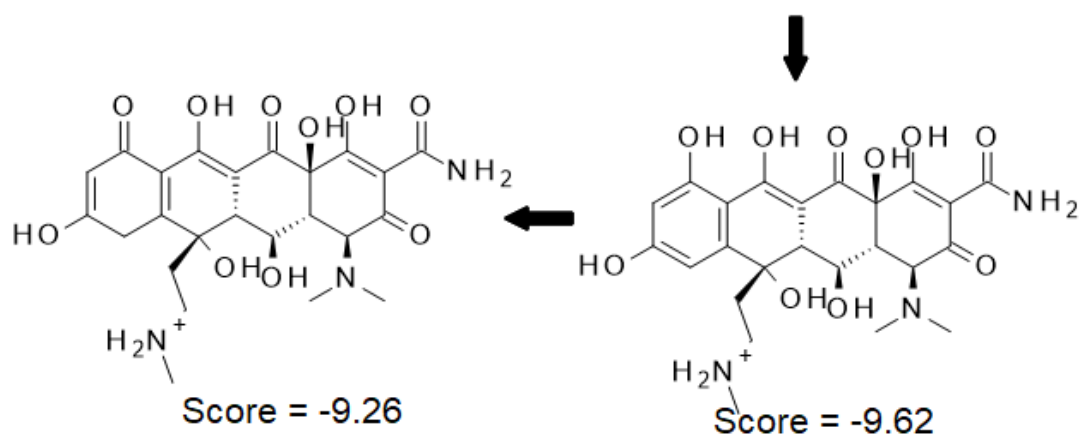
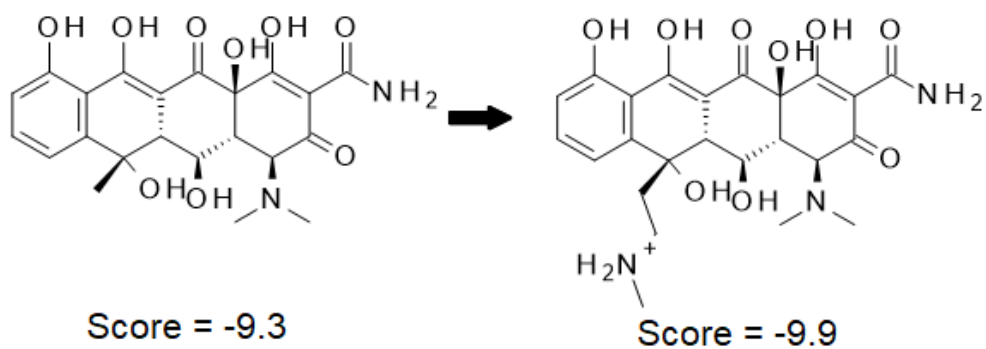


Fig. S7: Structure based drug design to optimize the potential inhibitory activity of oxytetracycline. Given scores are GVBI/WSA dG scores from docked complexes with 3Cl<sup>Pro</sup>.



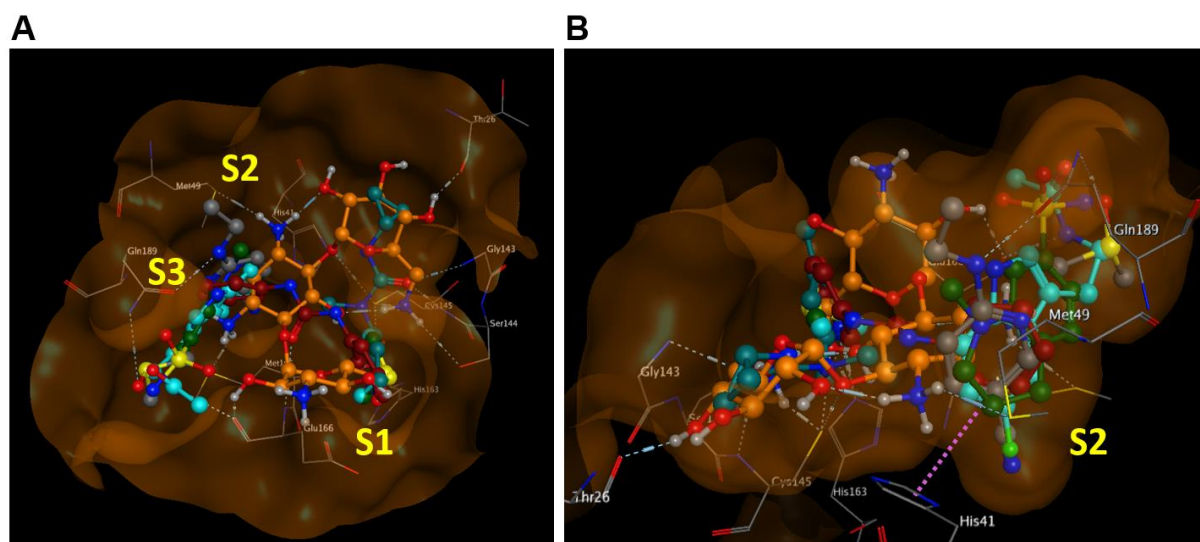


Fig. S8: Overlay of Kanamycin (orange) docked in this study and various non-covalent fragments, x0104 (S2, cyan), x0434 (dark brown), x0397 (blue green), x0195 (green), x0305 (gray) of very recent crystallographic fragment screen [1], within the binding pocket of 3CL<sup>pro</sup>. A) Top view on binding site with subpockets S1-S3. B) Side view particularly on S2 (right front) demonstrating that the aromatic group of 4 out of 5 fragments occupies the S2-sub-pocket and forms a T-shaped PI-stacking interaction with catalytic His41.

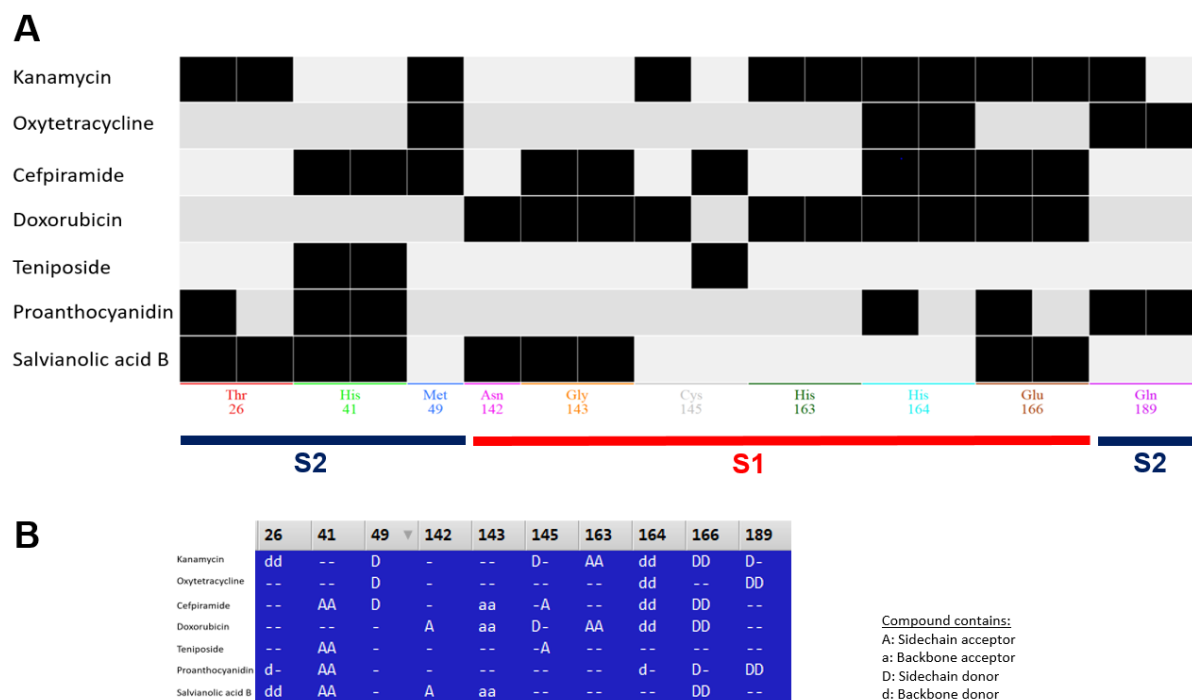
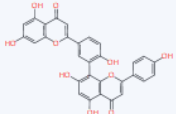
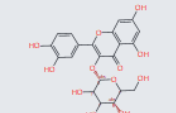
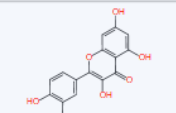
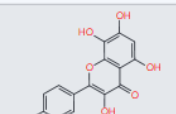
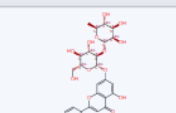
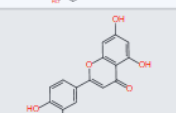
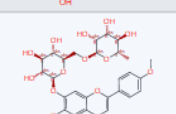
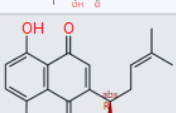
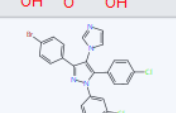
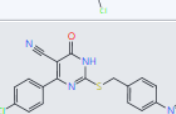
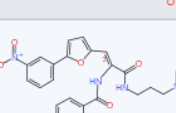
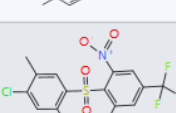
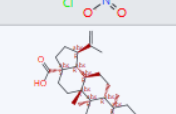
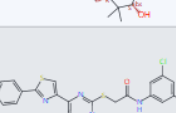
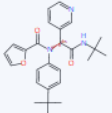
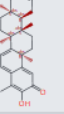
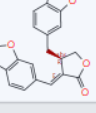
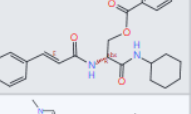
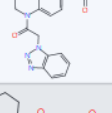
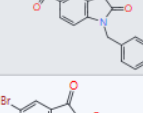
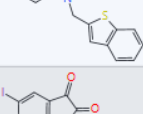
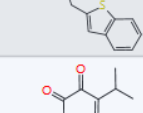
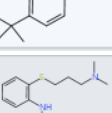
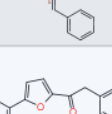
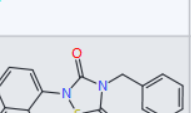
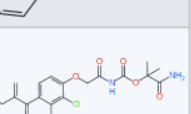
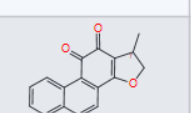
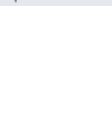


Fig. S9: Different patterns of protein-ligand interaction fingerprints (PLIFs) analysis within the active site of 3CL<sup>pro</sup>. A) PLIFs for indicated compounds showing the involved amino acids underneath. The interacting amino acids are assigned to sub-pockets S1 (red bar) or S2 (dark blue bar). B) Shows the type of interactions, in this case only H-bonds using a letter code that is explained in the legend in the right lower corner.

Table S1: Known inhibitors of 3CL<sup>pro</sup>

Structure	Name	London dG Score (MOE)	Vina Score	3CLpro_IC50 / $\mu\text{M}$	Literatur	Comment
	Biflavonoid 86	-15.225 (mean, n=40)	-9,6	8,3	Ryu, Y. B. Bioorg. Med. Chem. 2010, 18, 7940–7947.	Flavonoid
	Quercetin-3- $\beta$ -galactoside	-14.507 (mean, n=130)	-8,7	43	Chen, L Bioorg. Med. Chem. 2006, 14, 8295–8306.	Flavonoid
	Quercetin	-14.388 (mean, n=20)	-7,3	23,8	Chen, L Bioorg. Med. Chem. 2006, 14, 8295–8306.	Flavonoid
	Herbacetin	-14.081 (mean, n=10)	-7,5	33	Jo, S. (2020) J Enzyme Inhib Med Chem, 35, 145-151.	Flavonoid
	Rhoifolin	-13.918 (mean, n=20)	-9,1	28	Jo, S. (2020) J Enzyme Inhib Med Chem, 35, 145-151.	Flavonoid
	Luteolin	-13.808 (mean, n=20)	-7,4	10,6	Yi, L. J. Virol. 2004, 78, 11334–11339.	Flavonoid anti-oxidant, anti-inflammatory, apoptosis-inducing and chemopreventive
	Pectolarin	-12.75 (mean, n=20)	-8,6	38	Jo, S. (2020) J Enzyme Inhib Med Chem, 35, 145-151.	Flavonoid anti-inflammatory
	Shikonin	-11.66 (mean, n=20)	-7	16	DOI: 10.1101/2020.02.26.964882	
	134	-11.119 (mean, n=20)	-7,3	2,5	Kuo, C. J. FEBS Lett. 2009, 583, 549–555.	
	140	-11.08 (mean, n=20)	-8,3	6,1	Ramajayam, R. Bioorg. Med. Chem. Lett. 2010, 20, 3569–3572.	
	186	-11.04 (mean, n=20)	-8,1	9,1	Nguyen, T. T. H. Bioorg. Med. Chem. Lett. 2011, 21, 3088–3091.	
	103	-11.013 (mean, n=20)	-7,1	0,3	Lu, I.-L. J. Med. Chem. 2006, 49, 5154–5161.	
	Betulinic acid	-10.944 (mean, n=20)	-7,4	10	Wen, C.-C. J. Med. Chem. 2007, 50, 4087–4095.	
	105	-10.924 (mean, n=10)	-8,3	3	Tsai, K.-C. J. Med. Chem. 2006, 49, 3485–3495.	



Structure	Name	London dG Score (MOE)	Vina Score	3CLpro_IC50 / $\mu\text{M}$	Literatur	Comment
	ML188	-10.728 (mean, n=20)	-7,6	1,5	Jacobs, J. (2013) J Med Chem, 56, 534-46.	16-(S) enantiomer is inactive! competitive and non-covalent PDB 3V3M
	Iguesterin	-10.696 (mean, n=10)	-8,4	2,6	Ryu, Y. B. Bioorg. Med. Chem. Lett. 2010, 20, 1873-1876.	
	Savinin	-10.602 (mean, n=20)	-7,7	25	Wen, C.-C. J. Med. Chem. 2007, 50, 4087-4095.	
	SK23	-10.596 (mean, n=20)	-7,7	30	Konno, H. (2017) Bioorg Med Chem Lett, 27, 2746-2751.	
	ML300	-10.555 (mean, n=10)	-7,6	4,1	Turlington, M Bioorg. Med. Chem. Lett. 2013, 23, 6172-6177.	PPB Fu (h, r): 4.8%, 10.6% CL_hep (h,r): 20, 67 mL/min/kg CYPs ( $\mu\text{M}$ ): 7.7 (1A"),
	Isatin derivative 81	-10.454 (mean, n=20)	-7,9	1,0	Liu, W. Bioorg. Med. Chem. 2014, 22, 292-302.	
	Isatin derivative 78	-10.411 (mean, n=10)	-7,3	0,98	Liu, W. Bioorg. Med. Chem. 2014, 22, 292-302.	selective vs. Papain, chymotrypsin, trypsin
	Isatin derivative 80	-10.387 (mean, n=10)	-7,3	0,95	Liu, W. Bioorg. Med. Chem. 2014, 22, 292-302.	
	Tanshinon 7	-10.27 (mean, n=10)	-7	21	Park, J. Y. Bioorg Med Chem, 20, 5928-35.	
	Cinanserin	-10.199 (mean, n=20)	-6,5	125	DOI: 10.1101/2020.02.26.964882	serotonin antagonist with limited antihistaminic, anticholinergic, and immunosuppressive
	129	-10.175 (mean, n=20)	-7,4	13	Zhang, J. Bioorg. Chem. 2008, 36, 229-240.	non-covalent
	Tideglusib	-10.159 (mean, n=20)	-7,9	1,55	DOI: 10.1101/2020.02.26.964882	potent anti-inflammatory and neuroprotective that is a non-ATP competitive inhibitor of glycogen
	Etacrynic acid amide 74	-10.157 (mean, n=20)	-7,9	35,3	Kaepler J. Med. Chem. 2005, 48, 6832-6842	
	Tanshinon 6	-10.076 (mean, n=40)	-7,3	14,4	Park, J. Y. Bioorg Med Chem, 20, 5928-35.	

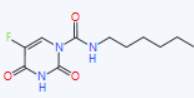
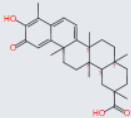
	Carmofur	-9.4159 (mean, n=20)	-6,4	1,8	DOI: 10.1101/2020.02.26. 964882	acute toxic antimetabolite (pyrimidine analogue) antineoplastic derivative of
	Celastrol			10,3	Ryu, Y. B. Bioorg. Med. Chem. Lett. 2010, 20, 1873–1876.	antioxidant and anti-inflammatory activity that may prevent neuronal degeneration

Table S2: Docking scores of best hits from pharmacophore search of ZINC15 library. The GVBI/WSA is a forcefield-based scoring function implemented in MOE software, which estimates the free energy of binding of the ligand from a given pose [2].

Cpd	GVBI/WSA dG (kcal/mol)
ZINC000008219992	<b>-8.8</b>
ZINC000096222891	-8.5
ZINC000096114417	<b>-9.3</b>
ZINC001570001158	-8.5
ZINC000016429284	-8.1
ZINC000015275997	<b>-9.5</b>
ZINC000218242102	<b>-8.8</b>

## References:

- [1] A. Douangamath, D. Fearon, P. Gehrtz, T. Krojer, P. Lukacik, C.D. Owen, E. Resnick, C. Strain-Damerell, A. Aimon, P. Ábrányi-Balogh, J. Brandaõ-Neto, A. Carbery, G. Davison, A. Dias, T.D. Downes, L. Dunnett, M. Fairhead, J.D. Firth, S.P. Jones, A. Keely, G.M. Keserü, H.F. Klein, M.P. Martin, M.E.M. Noble, P. O'Brien, A. Powell, R. Reddi, R. Skyner, M. Snee, M.J. Waring, C. Wild, N. London, F. von Delft, M.A. Walsh, bioRxiv, (2020) 2020.2005.2027.118117.
- [2] C.R. Corbeil, C.I. Williams, P. Labute, J Comput Aided Mol Des, 26 (2012) 775-786.